EurJIC
European Journal of Inorganic Chemistry

Research Article
doi.org/10.1002/ejic.202200335

Chemistry Europe
European Chemical Societies Publishing

www.eurjic.org

# Ligand Exchange Triggered Photosensitizers – Bodipy-Tagged NHC-Metal Complexes for Conversion of $^3O_2$ to $^1O_2$

Stepan Popov[a] and Herbert Plenio*[a]

A new imidazolium salt **3**·HI with 8-Bodipy as one N-aryl substituent was synthesized from 8-chloro-Bodipy and imidazole followed by alkylation with *i*PrI. NHC-metal complexes [CuCl(**3**)], [AuCl(**3**)], [Pd(allyl)Cl(**3**)] and [MCl(cod)(**3**)] and [MCl(CO)$_2$(**3**)] (M = Rh, Ir) were synthesized and the X-ray crystal structure of [IrCl(CO)$_2$(**3**)] determined. The donation of NHC **3** was determined via IR (ν(CO) and cyclic voltammetry (Ir(I/II) redox potential). The photosensitizing properties of the complexes for the generation of $^1O_2$ were quantified observing singlet oxygen quantum yield of up to $\Phi_{s.o.} = 0.63$. [IrCl(cod)(**3**)] displays poor $\Phi_{s.o.} = 0.09$, but, following a simple ligand exchange reaction of cod by two CO [IrCl(CO)$_2$(**3**)], a pronounced increase to $\Phi_{s.o.} = 0.63$ is observed.

## Introduction

The conjugation of ligands for organometallic chemistry with fluorophores (Bodipy) and the synthesis of the derived metal complexes generates compounds in which the fluorescence properties of the fluorophore can be modulated via chemical reactions in the coordination sphere of the respective transition metal. The simple ligand exchange reaction of 1,5-cyclooctadiene by two carbon monoxide at rhodium (Scheme 1a) is an example for such a fluorogenic reaction leading to a nearly to 100-fold increase in the fluorescence intensity.[1] The oxidative addition of $H_2$ by an Ir(I) complex results in a very pronounced increase in the fluorescence, since the initial Ir(I) shows only modest fluorescence quantum yield.[2] Even the generation of a "naked" gold cation by reaction of [AuCl(NHC)] with [Ag(NTf$_2$)] can be monitored by fluorescence spectroscopy since it leads to a small, but significant increase in fluorescence (Scheme 1c).[3] The same applies to the Pd-diimine complex (Scheme 1d) during the polymerization of ethene.[4]

Based on the observation of fluorescent and non-fluorescent complexes, the question arises as to what is happening, when the excitation energy is not converted into fluorescence. Obviously, numerous quenching pathways[5] can lead to the radiationless decay of the excited state,[6] but especially in the presence of heavy transition metals with strong spin-orbit coupling intersystem crossing to generate triplet states poses a feasible alternative.[7] The use of heavy atoms is the most popular method to enhance the intersystem crossing of organic compounds, and this approach has also been applied to numerous Bodipy derivatives (Scheme 2). The derived photosensitizers utilize the triplet state energy for the generation of $^1O_2$ from $^3O_2$.[8] Some important (transition metal-based) Bodipy-based examples of photosensitizers are shown in Scheme 2 for compounds A,[9] B,[10] C,[11] D,[12] E,[13] and F,[14] G[15] and H.[16] Other than using heavy atoms (iodine, transition metals),[17] more recently additional strategies such as orthogonal π-systems including Bodipy dimers[11,18] have evolved, which also lead to efficient photosensitizers useful in photodynamic therapy.[19]

Nonetheless, the modulation of the intersystem crossing and the photosensitizing ability normally relies on a modification of the covalent framework, which requires significant synthetic effort. It appears to be a more flexible approach to link the fluorophore to a ligand to which a number of different metals with variable ligand spheres can be coordinated and to monitor their influence on the photosensitizing properties. In order to maximize the impact of the metal center, the metal binding unit should be attached close to the fluorophore (Bodipy). Consequently, here the synthesis of complexes will be reported in which the imidazolylidene-metal complex is directly attached to the Bodipy core and the suitability of the respective complexes as photosensitizers for $^1O_2$ generation studied.

## Results and Discussion

### Synthesis of imidazolium salt and NHC-metal complexes

The reaction of meso-chloro Bodipy **1** with imidazole provides the respective Bodipy-substituted imidazole in 91% yield (Scheme 3). Alkylation of **2** with 2-iodopropane yields the imidazolium salt **3**·HI, which serves as a precursor for the synthesis of NHC-metal-complexes. There are three commonly employed approaches for the synthesis of such complexes:[20] a) in-situ synthesis of [AgX(NHC)] and transfer of the NHC from $Ag^+$ to a metal halide with precipitation of silver halide; b) deprotonation of an azolium salt to the respective carbene and

[a] S. Popov, Prof. Dr. H. Plenio
Organometallic Chemistry,
Technical University of Darmstadt,
Alarich-Weiss-Str. 12, 64287 Darmstadt, Germany
E-mail: herbert.plenio@tu-darmstadt.de

Supporting information for this article is available on the WWW under https://doi.org/10.1002/ejic.202200335

Research Article
doi.org/10.1002/ejic.202200335


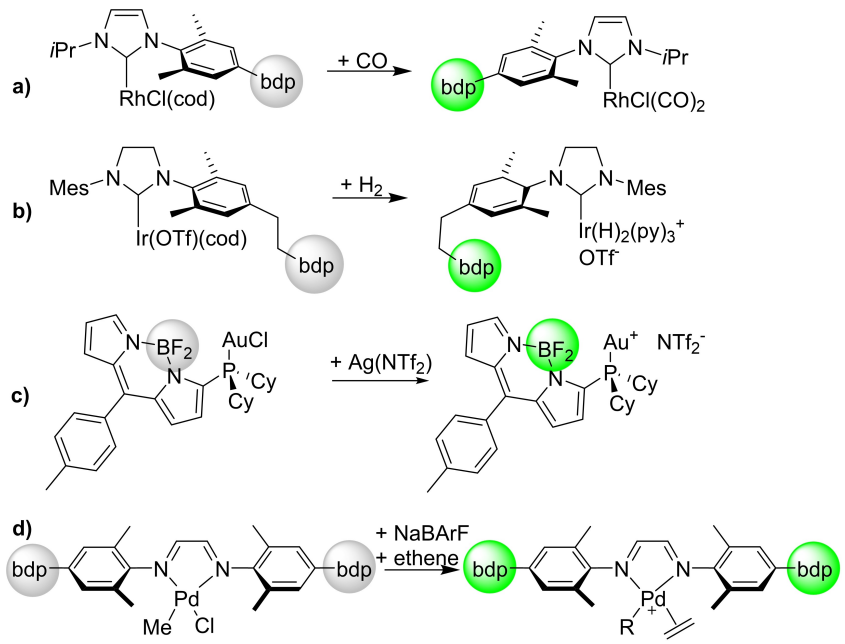


**Scheme 1.** Fluorogenic reactions involving Bodipy-tagged organometallic complexes (gray denotes weak fluorescence, green strong fluorescence).

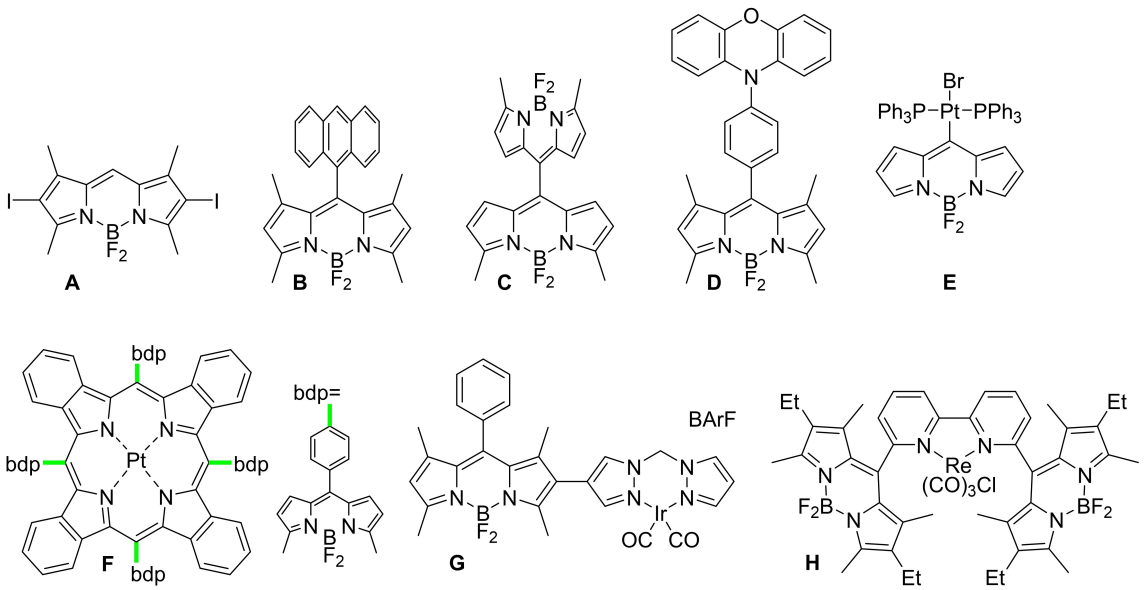


**Scheme 2.** Efficient (transition metal) Bodipy photosensitizers.

reaction with a metal complex; and c) the weak base approach[21] with the direct formation of NHC-metal complex from an azolium salt and metal complexes. For the synthesis of NHC-metal complexes utilizing carbene **3** both approaches b) and c) failed, probably since the basic reaction conditions led to the decomposition of the Bodipy subunit of the imidazolium salt **3**·HI. Method a) was successful even though several of the respective NHC-metal complexes were isolated in modest yields only.

All complexes display the same dark red color of the Bodipy unit, since the extinction coefficient of the fluorophore is much higher than that of the respective d-d-transition.

[IrCl(CO)$_2$(**3**)] was synthesized in virtually quantitative yield by bubbling CO gas through a solution of [IrCl(cod)(**3**)] in $CH_2Cl_2$. The analysis of the IR spectra, specifically of the respective $\nu$(CO), provides information on the donor properties of the respective NHC. In order to allow the comparison of the ATR data to the transmission IR data,[22] the data for the reference complex [IrCl(CO)$_2$(**IMes**)] ($\nu_{av}$(CO) = 2017 cm$^{-1}$) were also recorded using the same ATR-IR spectrometer.[23] The

Research Article
doi.org/10.1002/ejic.202200335



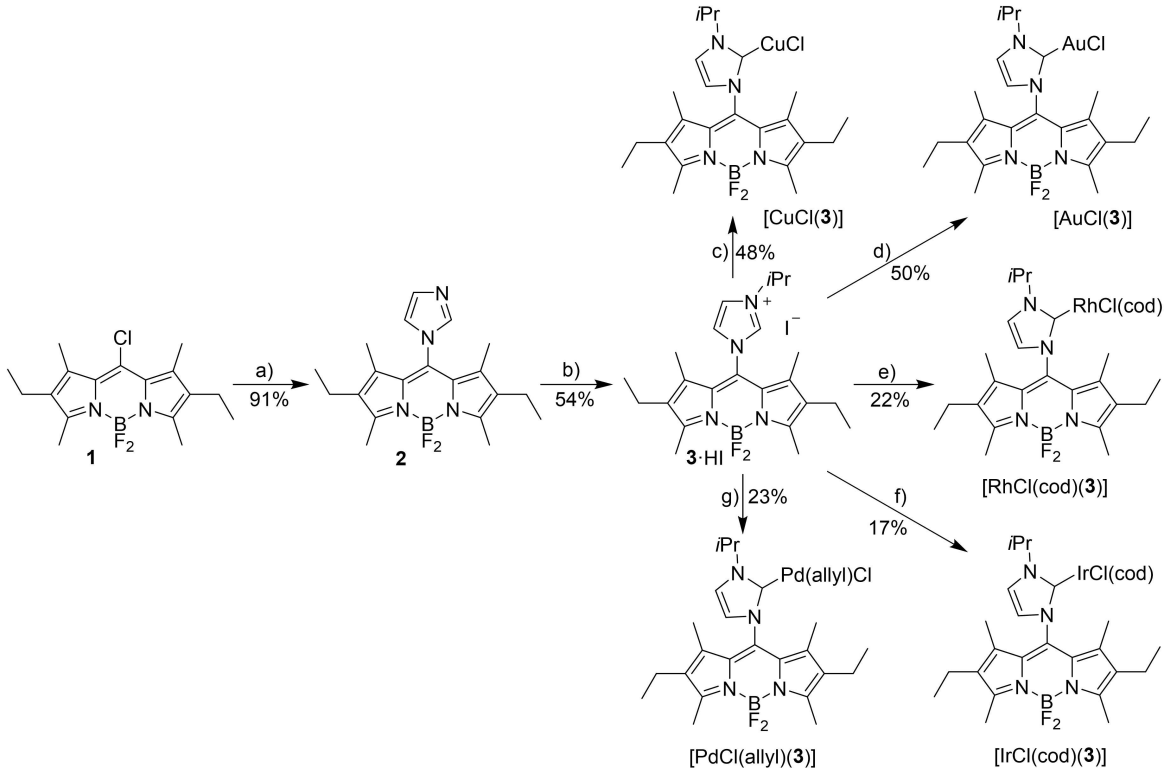


**Scheme 3.** Synthesis of Bodipy imidazolium salt **3**·HI and NHC metal complexes. Reagents and conditions: (a) potassium carbonate, imidazole, DCM, RT, 16 h; (b) 2-iodopropane, acetone, 70 °C, 24 h; (c) $Ag_2O$, DCE, 55 °C, 60 min; then CuCl, DCE, 60 °C, 1 h; (d) $Ag_2O$, DCE, 55 °C, 90 min; then [AuCl($Me_2S$)], DCE, 60 °C, 2 h; (e) $Ag_2O$, DCE, 55 °C, 90 min; then $[RhCl(cod)]_2$, DCE, 60 °C, 1.5 h; (f) $Ag_2O$, DCE, 55 °C, 90 min; then $[IrCl(cod)]_2$, DCE, 60 °C, 1 h min; (g) $Ag_2O$, DCE 55 °C, 90 min; then $[Pd(allyl)Cl]_2$, DCE, 60 °C, 1.5 h.

$\nu_{av}$(CO) for [IrCl(CO)$_2$(**3**)] (2013 cm$^{-1}$)(Figure S51) are shifted by −4 cm$^{-1}$ relative to those of the reference complex. Based on these data, NHC **3** appears to be more electron-donating than the reference carbene IMes. With a view to the electron-accepting properties of the Bodipy unit this is unexpected.[24] Furthermore replacing the N-mesityl group by an *i*Pr group was shown to have very little influence on the donation of the respective NHC ligand.[19c] Alternatively, the redox potential Ir(I/II) in [IrCl(cod)(**3**)] also provides information on the donor ability of the NHC ligands. [IrCl(cod)(**3**)] is characterized by a reversible cyclic voltammogram with $E_{1/2} = +0.811$ V for Ir(I/II). This redox potential indicates, that NHC **3** is significantly less electron-releasing than the reference NHC in [IrCl(cod)(**IMes**)] ($E_{1/2} = +0.759$ V). Obviously this result is not in accord with the IR data. However, based on the ewg nature of the Bodipy group, it was expected that NHC **3** is less donating than IMes. Recently we also observed that for the related N,N′-dialkyl-substituted NHC [IrCl(CO)$_2$(**NHC**)] the ν(CO) data also deviate from the electronic information obtained via redox potentials.[19c] Based on the data presented here and our previous experience it is our opinion,[25] that Ir(I/II) redox potentials are the more reliable parameter for the determination of NHC donicity.[26] This is based on the following other observations: a) IR data depend very much on the measurement conditions and for transmission data the nature of the solvent has a pronounced influence on the ν(CO), for ATR-IR the nature of the probe (refractive index) has a very strong influence on the observed wavenumbers and it is advisable to measure against a standard complex; b) the signal dispersion in (NHC)MX(CO)$_2$ complex is relatively small compared to the resolution of routine spectrometers, while redox potentials derived from reversible cyclic voltammograms the signal dispersion can be up to 100-times higher than the experimental error of the redox potential determination.

### X-ray crystal structure of [IrCl(CO)$_2$(3)]

In order to probe the structure of [IrCl(CO)$_2$(**3**)] in more detail and to potentially resolve the inconsistency in the *ν*(CO) data, single crystals of [IrCl(CO)$_2$(**3**)] were grown by cooling a pentane/$CH_2Cl_2$ solution of the complex (Figure 1). The crystal structure was solved and refined with SHELXT[27] within the OLEX2 shell.[28] The Ir(I) displays the typical square-planar coordination sphere consisting of two cis-CO-ligands, a chloride and the carbene carbon. Both the imidazolylidene and the Bodipy are planar units and as a consequence of the methyl groups in the 1,7-position of Bodipy the planes of the Bodipy and the imidazolylidene are orthogonal. Bond lengths and angles are in the typical range observed for such complexes.[29] The Ir–C(NHC) bond is on the shorter side of the typical distances which range from 206 −211 pm.[29b] Boron resides in an almost ideal tetrahedral environment and the respective

Research Article
doi.org/10.1002/ejic.202200335


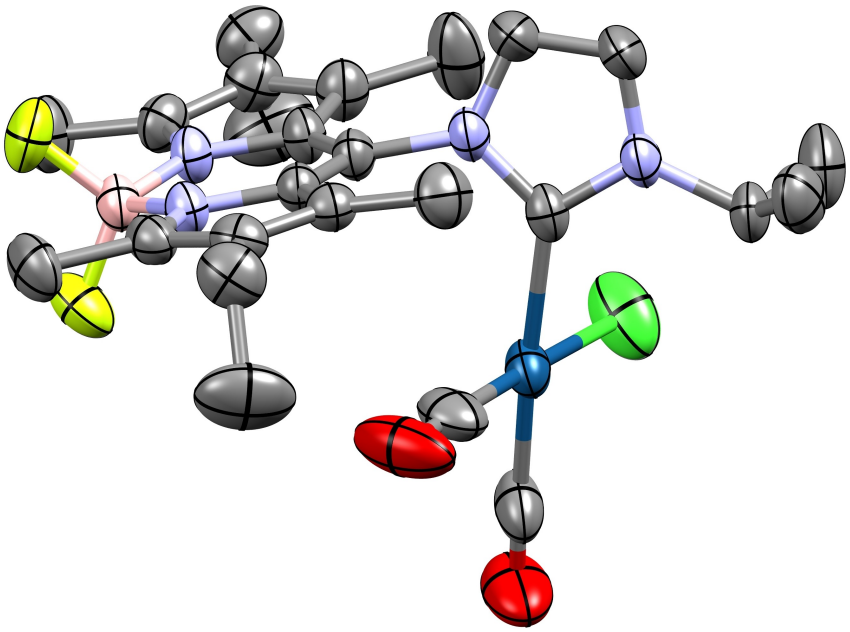

**Figure 1.** Crystal structure of [IrCl(CO)$_2$(**3**)] (ORTEP plot, hydrogen atoms omitted, CCDC-2174553). Relevant bond lengths (pm) and angles (°): Ir–C(NHC) 206.3(4), Ir–CO (186.6(5), 181.4(6), Ir–Cl (234.7(1), C(NHC)-Ir–C 178.2 (1), 93.4(2), C(NHC)-Ir–Cl 88.5(1), B–F (137.1(5), 138.9(5).

angles of boron, nitrogen and fluorine are within two degrees of 109°. A slightly unusual structural feature is the ca. 20° deviation from perfect orthogonality of the square-planar Ir environment and the imidazolylidene plane. The origin of this tilting appears to be the larger steric bulk of the chloride compared to the carbonyl ligand.[30] The rotation of the square-planar unit around the Ir–C(NHC) axis relieves the close contact of the chloride with the 1,7-Bodipy methyl groups, which are shielding the space on both sides of the imidazolylidene unit.

## Singlet oxygen generation

Important spectroscopic data like absorption and emission maxima, fluorescence quantum yield ($\Phi_{em}$) and $^1O_2$ quantum yields ($\Phi_{s.o.}$) and extinction coefficients for the newly synthesized complexes (Scheme 3) as well as for other complexes from previous studies (Scheme 4)[1–3,31] are summarized in Table 1.

The UV/Vis spectra of the new transition metal complexes are dominated by the Bodipy absorption at around 540 nm. Relative to the imidazolium salt ($\lambda_{max}$ = 545 nm) the absorption maxima experience a modest hypsochromic shift of between 4–7 nm depending on the metal. The extinction coefficients of the metal complexes range from 23.000 $M^{-1}cm^{-1}$ up to 75.000 $M^{-1}cm^{-1}$. On the lower end are the two [MCl(CO)$_2$(**3**)] (M = Ir, Rh) complexes while the three gold complexes display the highest extinction coefficients. The emission wavelengths also experience a small hypsochromic shift relative to **3**·HI ($\lambda_{em}$ = 558 nm) ranging between 549–554 nm for the different metal complexes. Among the recently reported complexes those with two Bodipy units display the highest extinction coefficients.

The differences in fluorescence quantum yields for the compounds reported here are much more pronounced. While the two [MCl(cod)(**3**)] (M = Ir, Rh) complexes display negligible fluorescence, the related [MCl(CO)$_2$(**3**)] (M = Ir, Rh) show stronger emissions with $\Phi_{em}$ = 0.17 and 0.09. This fluorescence gain is typical for such complexes upon replacement of a 1,5-

**Table 1.** Photophysical and photochemical parameters for the photosensitizers. Singlet oxygen quantum yield ($\Phi_{s.o.}$) was determined in $CH_3CN$ solution by monitoring the decay of DPBF ($c_0$ = 90 μM) in a presence of the corresponding photosensitizer ($c$ = 1.0 μM) using 2,6-diiodo-Bodipy as a reference in $CH_3CN$ ($\Phi^{st}_{s.o.}$ = 0.75).[4]

| Compound | $\lambda_{abs,max}$ | $\lambda_{em,\ max}$ | $\Phi_{em}$ | $\Phi_{s.o.}$ | $\varepsilon$ |
|---|---|---|---|---|---|
| **3**·HI[a] | 545 | 558 | 0.45 | 0.11 | 64 |
| [AuCl(**3**)][a] | 538 | 549 | 0.28 | 0.43 | 75 |
| [AuNTf$_2$(**3**)][a] | 538 | 549 | 0.21 | 0.46 | 73 |
| [Pd(allyl)Cl(**3**)][a] | 536 | 549 | 0.23 | 0.46 | 59 |
| [CuCl(**3**)][a] | 535 | 554 | 0.025 | 0.11 | 51 |
| [RhCl(CO)$_2$(**3**)][a] | 540 | 554 | 0.009 | 0.12 | 33 |
| [IrCl(CO)$_2$(**3**)][a] | 540 | 554 | 0.017 | 0.63 | 23 |
| [IrCl(cod)(**3**)][a] | 541 | – | < 0.01 | 0.09 | 39 |
| [RhCl(cod)(**3**)][a] | 541 | – | < 0.01 | 0.26 | 56 |
| [IrCl(cod)(NHC_PK1)] | 506 | 530 | 0.008 | 0.18 | 67 |
| [IrCl(cod)(NHC_PK2)] | 510 | 524 | 0.022 | 0.035 | 85 |
| [AuCl(NHC_PK)] | 506 | 529 | 0.70 | 0.051 | 65 |
| [AuCl(NHC_OH1)] | 526 | 538 | 0.67 | 0.065 | 95 |
| [IrCl(cod)(NHC_OH1)] | 526 | 538 | 0.060 | 0.074 | 94 |
| [AuCl(Cy$_2$P-bdp)] | 510 | 526 | 0.096 | 0.022 | 44 |

Absorption ($\lambda_{abs}$) and emission ($\lambda_{em}$) maxima and fluorescence quantum yield ($\Phi_{em}$) are given according to the previously reported complexes. The molar absorption coefficients ($\varepsilon$ $10^3$ $M^{-1}cm^{-1}$) were determined for the respective photosensitizers in $CH_3CN$ solution ($c$ = 1.0 μM). [a] The value of fluorescence quantum yield was determined in $CH_3CN$ solution using rhodamine 6G as a standard fluorophore ($\Phi_{st}$ = 0.95 in EtOH).

Research Article
doi.org/10.1002/ejic.202200335


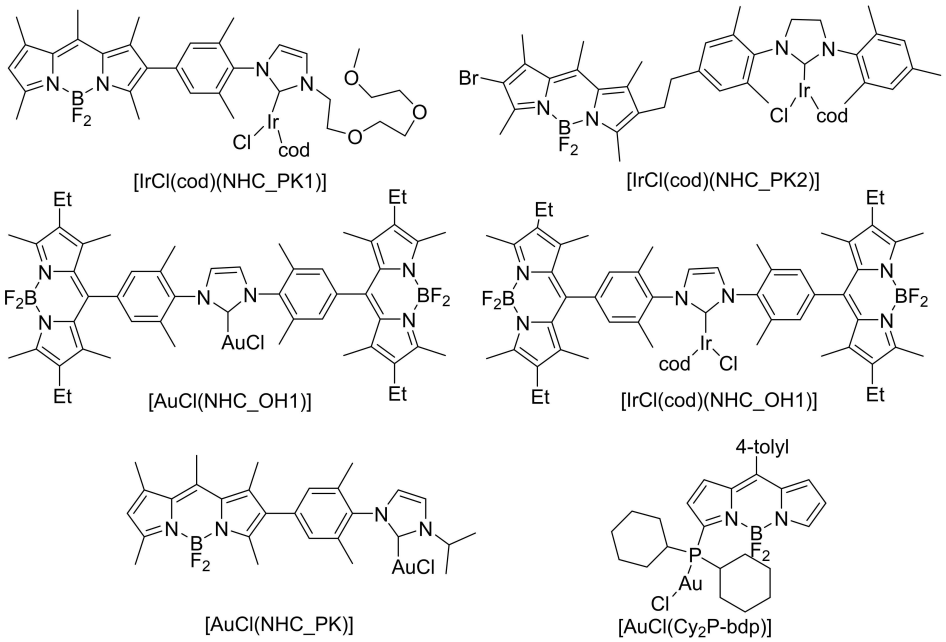


**Scheme 4.** Previously reported complexes included in the present studies.

cyclooctadiene ligand by two carbonyls and this fluorogenic reaction has been used for the detection of CO.[1,31a,32] The remaining 4d- and 5d-metal complexes with NHC **3** display quantum yields in the narrow range between 0.21–0.28. Compared to related metal complexes reported previously (the complexes listed in the bottom half of Table 1 serve as an example),[1] the fluorescence quantum yields of the metal complexes with NHC **3** are significantly lower and it is interesting to learn why this is the case. In the context of earlier results two pathways are conceivable – either the excitation energy is lost via PET-quenching[6a] (electron-transfer from the Bodipy excited state to the metal center followed by by a non-radiative recombination of the charges) or the close vicinity of heavy transition metals with strong spin-orbit coupling and the fluorophore facilitates intersystem crossing and a significant transfer of the excitation energy into the triplet state.[7]

The generation of $^1O_2$ was quantified using the cyclo-addition reaction with 1,3-Diphenylisobenzofurane (DPBF)[33] by monitoring the decrease of the 410 nm DPBF absorbance with time via UV/Vis-spectroscopy (Figure 2, left). A typical linear plot of absorbance vs. time is shown in Figure 2 (right) as an example of the corresponding zero-order reaction and the slope is used to calculate the singlet oxygen quantum yield $\Phi_{s.o.}$.[34,33] The respective $\Phi_{s.o.}$ was determined for all complexes listed in

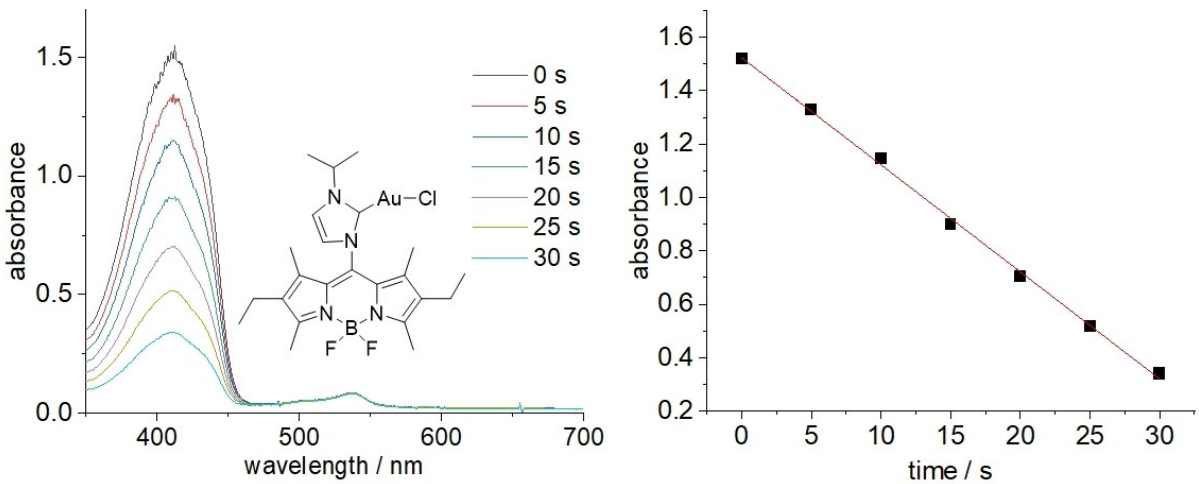


**Figure 2.** Decay of the 410 nm absorbance of DPBF ($c_0 = 90$ μM) in the presence of [AuCl(**3**)] ($c = 1.0$ μM) in $CH_3CN$ and irradiation with a green LED and plot of absorbance vs. time.

Research Article
doi.org/10.1002/ejic.202200335


Table 1. The expectation being that the proximity of a heavy atom and the fluorophore increases the likelihood of intersystem crossing – the closer the contact the higher the photosensitizer ability.

There is no evidence for the oxidation of transition metal (complexes) by $^1O_2$ during the photosensitizing experiments in any of the studied complexes. While this appears to be difficult for the Au(I) and the Pd(II) complexes anyway, it might be possible for [IrCl(cod)(**3**)] with an Ir(I/II) redox potential of +0.84 V. The redox potential of the electron-deficient [IrCl(CO)$_2$(**3**)] cannot be easily determined due to the lability of the oxidized species (CO dissociation), but is expected to be approx. +500 mV anodic of the Ir(I/II) redox potential for [IrCl(CO)$_2$(**3**)].[1] However, even for the Ir complexes, the UV/Vis and the fluorescence spectra of the metal complexes remain unchanged during the singlet oxygen generation and based on this oxidation of the metal complexes is unlikely.

With a single exception, all complexes in which the Bodipy unit is spatially separated from the transition metal are poor photosensitizers with an inefficient $^1O_2$ formation. The only exception being complex [IrCl(cod)(NHC_PK1)] with $\Phi_{s.o.}=0.18$. Despite small $\Phi_{s.o}$ several of the complexes in Scheme 4 also display modest fluorescence quantum yields and it is thus likely, that the excitation energy is lost via PET quenching.[6a] Interestingly, in complex [AuCl(Cy$_2$P-bdp)] the gold is bonded very close to the Bodipy core, but both fluorescence and $^1O_2$ quantum yields are poor. Again, it seems that the excitation energy is predominantly channeled into PET quenching, which also appears to be the case for [MCl(cod)(**3**)] (M = Rh, Ir). The remaining complexes with NHC **3** (Table 1) display modest $\Phi_{em}$ of below 0.30, but at the same also act as efficient photosensitizers - depending on the nature of the transition metal. The gold complex is more efficient than the lighter copper complex, and the same applies to the iridium relative to the lighter rhodium complex. The iridium complex is useful for the generation of $^1O_2$ and at $\Phi_{s.o.}=0.63$ rivals the performance of the 2,6-diiodo-Bodipy. It is very interesting, that a simple ligand exchange reaction replacing the 1,5-cyclooctadiene ligand in [IrCl(cod)(**3**)] with two CO ligands generates the efficient photosensitizer [IrCl(CO)$_2$(**3**)]. Based on the recent concept of $S_1$-$T_1$ tuning,[35] it is assumed that a smaller energy difference between the $S_1$ and the $T_1$ state in [IrCl(CO)$_2$(**3**)] enables facile intersystem crossing in this complex. Nonetheless, the singlet oxygen quantum yield depends on numerous factors, not just the rate of the intersystem crossing $k_{isc}$ but also the rates of radiative and non-radiative decay of excited states relative to $k_{isc}$ and the thermal accessibility of excited d-states enabling non-radiative deactivation pathways[36] and the efficient transfer of the $T_1$ energy to $^3O_2$.[33] In this complicated interplay of different factors minor changes in the molecular setup can result in significant changes of the properties.

The cod-to-CO ligand exchange reaction is very fast even at very low concentration of the complexes and tends to be virtually quantitative.[1,37] Previously, this reaction was identified as a fluorogenic reaction.[1] For [IrCl(cod)(**3**)] the cod-to-CO ligand exchange triggers the photosensitizer. A poor $^1O_2$ generating complex ($\Phi_{s.o.}=0.09$) is converted into an efficient photosensitizer ($\Phi_{s.o.}=0.63$) following the addition of two equivalents of CO to [IrCl(cod)(**3**)].

## Photooxidation of p-bromothioanisole

Finally, we were interested whether good photosensitizing properties of the respective transition metal complexes translate into good photocatalytic properties. The photooxidation of *p*-bromothioanisole to the respective sulfoxide (Scheme 5) was chosen as an exemplary reaction and substrate conversion determined by NMR spectroscopy.[38]

The photoreactor for the generation of $^1O_2$ was also used in the photocatalytic reactions and all reactions were carried out at 1 mol% loading of the metal complex (20 h reaction time). As expected, the poor photosensitizer [IrCl(cod)(**3**)] produced modest amounts of the sulfoxide (35% after 20 h), while the very efficient photosensitizer [IrCl(CO)$_2$(**3**)] provides substantially more product >99% after 20 h (40% after 8 h). At 66% conversion the gold complex [AuCl(**3**)] is reasonably efficient. Based on these results we reasoned that the catalytic role of the metal in such oxidation reactions is not limited to $^1O_2$ generation, since the higher affinity of gold towards sulfur might be one reason for better substrate conversion. Based on this argument, the accessibility of gold will be much better when the strongly coordinating chloride is replaced by a weakly coordinating bis-triflimidate $NTf_2^-$ and consequently the catalytic efficiency should increase. [Au(NTf$_2$)(**3**)] turns out to be much more active and provides virtually quantitative substrate conversion of >99% after only 9 h reaction time. These experiments support the hypothesis by Messerle et al.[15b] that the transition metal promotes the catalytic transformation of the thioanisole via metal-($O_2$) or metal-S interactions. Reactions of $^3O_2$ and $^1O_2$ with iridium complexes have been reported,[39] however, such Ir(I) complexes, appear to be significantly more electron-rich than [IrCl(CO)$_2$(**3**)][40] and there is no evidence (vide supra), that $^1O_2$ reacts with the complexes reported here. Gold complexes are better known for their interaction with sulfur than with oxygen and it is likely that the role of gold is twofold: spin-orbit coupling leads to efficient $^1O_2$ generation and coordination of substrate stabilizes the sulfur containing species (intermediates).

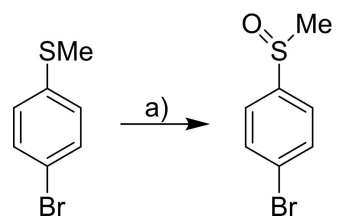


**Scheme 5.** Photooxidation of thioethers to the respective sulfoxides. Reagents and conditions: a) *t*-amyl alcohol, acetonitrile (1:1), green LED, photosensitizer.

Research Article
doi.org/10.1002/ejic.202200335



## Conclusions

It was shown that the simple modification of metal complex fragments bonded to an NHC ligand allows the modification of the fluorescence quantum yield and of the singlet oxygen fluorescence quantum yield. NHC-metal complexes with 3d- or 4d-metals (Cu, Rh) and weak spin-orbit coupling provide photosensitizers with modest activity only, while the binding of 5d-metals (Ir, Au) by NHC ligand **3** can provide efficient photosensitizers for the generation of $^1O_2$. However, based on the results reported here, the electronic structure of the transition metal also influences the ability to act as a photosensitizer. The electron-rich [IrCl(cod)(**3**)] turns out to be a much less efficient photosensitizer than [IrCl(CO)$_2$(**3**)], which is synthesized in virtually quantitative yield by a simple cod-to-CO ligand exchange. The ability to efficiently generate $^1O_2$ is not the only factor determining the reactivity of photosensitizers. In the oxidation of *p*-bromothioanisole, it may not even be the most important one.

## Experimental Section

***General experimental.*** Synthesis was performed in pre-dried Schlenk flasks under a positive pressure of argon or nitrogen. The flasks were fitted with rubber septa and gas-tight syringes with stainless steel needles or double-cannula were used to transfer air- and moisture-sensitive liquids.

***Instrumentation.*** $^1$H, $^{19}$F, and $^{13}$C-NMR spectra were recorded on a Bruker DRX 500 or Bruker ARX 300 spectrometer. The chemical shifts are given in parts per million (ppm) on the delta scale ($\delta$) and are referenced to tetramethylsilane ($^1$H, $^{13}$C-NMR = 0.0 ppm), the residual peak of $CHCl_3$ ($^1$H-NMR = 7.26 ppm, $^{13}$C-NMR = 77.16 ppm), the residual peak of $CH_2Cl_2$ ($^1$H-NMR = 5.32 ppm, $^{13}$C-NMR = 53.5 ppm) or hexafluorobenzene ($^{19}$F-NMR = -164.90 ppm). Abbreviations for NMR data: s = singlet; d = doublet; t = triplet; q = quartet; m = multiplet; bs = broad signal. Mass spectra were recorded on the Bruker Impact II using electron ionization (EI) and atmospheric-pressure chemical ionization (APCI). UV-Vis spectra were recorded on Analytik Jena Specord 600 UV-Vis spectrometer, fluorescence spectra were recorded on J&M TIDAS S700/CCD UV/NIR 2098 spectrometer combined with J&M TIDAS LSM monochromator with 75 W Xenon light source and thermo-controlled cuvette holder. Samples for emission and absorption measurements were contained in a 1 cm·1 cm quartz cuvette (Hellma Analytics). Cyclic voltammetry was performed using standard electrochemical instrumentation consisting of an EG&G 273A-2 potentiostat-galvanostat. A three-electrode configuration was employed. The working electrode was a Pt disk (diameter 1 mm) sealed in soft glass with a Pt wire as a counter electrode. The pseudo reference electrode was an Ag wire. Potentials were calibrated internally against the formal potential of ferrocene (+0.46 V vs. Ag/AgCl). All cyclic voltammograms were recorded in dry methylene chloride under an atmosphere of argon, supporting electrolyte N*n*Bu$_4$PF$_6$ ($c$ = 0.1 mol/L) at scan rate of 50-150 mV/s. The photoreactions were performed using a green LED light strip (12 V strip green light 5 m 3528 SMD 300 LED, 60 LED/m, 4.8 W per meter strips). Home-built photoreactor was made by wrapping approximately 2.3 m of the LED strips around a 600 ml glass beaker. The quartz cuvettes were placed in the middle of the photoreactor, with a bottom diameter of 9 cm for the beaker reactor.

**8-Imidazolo-Bodipy (2)**. In a 25 mL round-bottom flask equipped with a stirring bar, imidazole (502 mg, 7.38 mmol, 10 eq), 8-chloro-Bodipy **1** (250 mg, 0.74 mmol, 1 eq) and $K_2CO_3$ (407 mg, 2.95 mmol, 4 eq) were dissolved in DCM (10 ml). The mixture was stirred in a flask at room temperature for 24 h. The resulting solution was poured into DCM (200 mL). The organic layer was separated and was washed with water. After drying over $MgSO_4$, filtration, and evaporation. The crude product was purified by column chromatography (DCM : MeOH 25 : 1) to the product as a microcrystalline red solid (255 mg, yield 93 %).$^1$H NMR (300 MHz, chloroform-*d*) δ 7.57 (s, 1H, NCHN), 7.32 (s, 1H, CH), 7.01 (s, 1H, CH), 2.53 (s, 6H, $CH_3$ Bodipy), 2.33 (q, $J$ = 7.6 Hz, 4H, $\underline{CH_2}CH_3$ Bodipy), 1.41 (s, 6H, $CH_3$ Bodipy), 1.01 (t, $J$ = 7.6 Hz, 6H, $CH_2\underline{CH_3}$ Bodipy). $^{13}$C{$^1$H}c NMR (126 MHz, chloroform-*d*) δ 157.2, 137.5, 136.5, 134.2, 131.4, 130.8, 129.6, 119.9, 17.1, 14.6, 12.9, 8.8. $^{19}$F NMR (471 MHz, chloroform-*d*) δ −144.63 (dq, $J$($^{11}$B-$^{19}$F$_a$) = 33 Hz, $J$($^{19}$F-$^{19}$F) = 104 Hz), −145.39 (dq, $J$($^{11}$B-$^{19}$F$_b$) = 31 Hz, $J$($^{19}$F-$^{19}$F) = 108 Hz). HRMS (ESI positive): m/z calcd. for $C_{20}H_{26}BF_2N_4$: 371.22131 [M + H]; found 371.22155.

**Bodipy-imidazolium salt (3·HI)**. To the imidazole **2** (100 mg, 0.27 mmol, 1 eq) in 4 mL of acetone, 2-iodopropane (0.4 mL, 4 mmol, 15 eq) was added and the mixture was stirred in the sealed flask at 70 °C overnight. The mixture was cooled to room temperature, after removal of the volatiles, the residue was purified by column chromatography (10 : 1 DCM : MeOH) to give the product (79 mg, 54 % yield) as red microcrystalline solid. $^1$H NMR (500 MHz, chloroform-*d*) δ 10.39 (s, 1H, NCHN), 8.36–8.35 (m, 1H, CH), 7.43–7.42 (m, 1H, CH), 5.65–5.57 (m, 1H, CH *i*Pr), 2.49 (s, 6H, $CH_3$ Bodipy), 2.30 (q, $J$ = 7.6 Hz, 4H, $\underline{CH_2}CH_3$ Bodipy), 1.67 (d, $J$ = 6.7 Hz, 6H, $CH_3$ *i*Pr), 1.47 (s, 6H, $CH_3$ Bodipy), 0.99 (t, $J$ = 7.6 Hz, 6H, $CH_2\underline{CH_3}$ Bodipy). $^{13}$C{$^1$H} NMR (126 MHz, chloroform-*d*) δ 159.7, 136.2, 136.0, 135.6, 128.1, 126.2, 123.8, 122.9, 54.7, 23.5, 17.1, 14.5, 13.1, 9.7. $^{19}$F NMR (471 MHz, chloroform-*d*) δ −144.66 (dq, $J$($^{11}$B-$^{19}$F$_a$) = 33 Hz, $J$($^{19}$F-$^{19}$F) = 104 Hz), −145.41 (dq, $J$($^{11}$B-$^{19}$F$_b$) = 31 Hz, $J$($^{19}$F-$^{19}$F) = 108 Hz). $^{19}$F {$^{11}$B} NMR (471 MHz, chloroform-*d*) δ −144.38, −144.61, −145.50, −145.72. $^{11}$B NMR (160 MHz, chloroform-*d*) δ 0.48. HRMS (ESI positive): m/z calcd. for $C_{23}H_{32}BF_2N_4$: 413.26826 [M]; found 413.26888.

**General procedure A for the synthesis of metal complexes**. To a Schlenk flask equipped with a stirring bar containing **3**·HI and $Ag_2O$ under a flow of the nitrogen gas, dry 1,2-dichloroethane was added and the flask was sealed. After 90 min of stirring in the dark at 55 °C, a metal precursor was added, and the mixture was stirred for an additional 2 h at 60 °C. The resulting suspension was filtered through a short pad of celite. The filtrate was collected and evaporated under reduced pressure. The product was purified by column chromatography (cyclohexane/ethyl acetate 3 : 1).

**[AuCl(3)]**. Complex [AuCl(**3**)] was synthesized according to general procedure A. **3**·HI (50 mg, 0.092 mmol), $Ag_2O$ (10.7 mg, 0.046 mmol), [AuCl($SMe_2$)] (27.1 mg, 0.092 mmol) in 1,2-dichloroethane (5 mL). Complex [AuCl(**3**)] was obtained as a red microcrystalline solid (29 mg, 48 % yield). $^1$H NMR (500 MHz, chloroform-*d*) δ 7.32 (s, 1H, CH), 7.06 (s, 1H, CH), 5.31–5.22 (m, 1H, CH *i*Pr), 2.53 (s, 6H, $CH_3$ Bodipy), 2.33 (q, $J$ = 7.6 Hz, 4H, $\underline{CH_2}CH_3$ Bodipy), 1.57 (s, 3H, $CH_3$ *i*Pr), 1.49 (s, 6H, $CH_3$ Bodipy), 1.43 (s, 3H, $CH_3$ *i*Pr), 1.03 (t, $J$ = 7.6 Hz, 6H, $CH_2\underline{CH_3}$ Bodipy). $^{13}$C{$^1$H} NMR (126 MHz, chloroform-*d*) δ 172.0, 158.0, 136.3, 134.5, 131.9, 129.1, 122.6, 118.1, 54.4, 23.8, 23.6, 17.2, 14.6, 9.6. $^{19}$F NMR (471 MHz, chloroform-*d*) δ −144.11 (dq, $J$($^{11}$B-$^{19}$F$_a$) = 33 Hz, $J$($^{19}$F-$^{19}$F) = 108 Hz), −146.35 (dq, $J$($^{11}$B-$^{19}$F$_b$) = 31 Hz, $J$($^{19}$F-$^{19}$F) = 108 Hz). HRMS (APCI): m/z calcd. for $C_{23}H_{31}AuBClFN_4$: 625.19745 [M]; found 625.19859.

10 mL Schlenk flask was equipped with a stirring bar, the corresponding [AuCl(**3**)] (12.3 mg, 0.019 mmol) and [Ag($NTf_2$)] (7.8 mg, 0.020 mmol), followed by addition of $CH_2Cl_2$ (2 mL). The mixture was stirred for 2 h at room temperature, protected from

light. The formed precipitate of AgCl was separated by filtration over celite. The celite was washed with dichloromethane (10 mL). The combined filtrates were evaporated and dried overnight in a vacuum and obtained material was used further without additional purification.

**[IrCl(cod)(3)]**. Complex [IrCl(cod)(**3**)] was obtained according to general procedure A. **3**·HI (30 mg, 0.055 mmol), $Ag_2O$ (6.4 mg, 0.028 mmol), $[IrCl(cod)]_2$ (18.5 mg, 0.028 mmol) in 1,2-dichloroethane (2 mL) yields the complex as a dark red crystalline solid (7 mg, 17% yield). $^1$H NMR (500 MHz, chloroform-*d*) δ 7.18 (d, *J* = 2.0 Hz, 1H, CH), 6.97 (d, *J* = 1.9 Hz, 1H, CH), 5.85–5.80 (m, 1H, CH *i*Pr), 4.60–4.57 (m, 1H, $H_{cod}$), 4.31–4.26 (m, 1H, $H_{cod}$), 3.29–3.27 (m, 1H, $H_{cod}$), 2.77–2.73 (m, 1H, $H_{cod}$), 2.54 (d, *J* = 9.6 Hz, 6H, $CH_3$ Bodipy), 2.33 (q, *J* = 8.0 Hz, 4H, $\underline{CH_2}CH_3$ Bodipy), 2.26–2.15 (m, 2H, $H_{cod}$), 2.11–2.03 (m, 1H, $H_{cod}$), 1.96–1.87 (m, 1H, $H_{cod}$), 1.83–1.75 (m, 1H, $H_{cod}$), 1.74 (s, 3H, $CH_3$ *i*Pr), 1.56 (d, *J* = 6.8 Hz, 3H, $CH_3$ Bodipy), 1.52 (d, *J* = 6.8 Hz, 3H, $CH_3$ Bodipy), 1.41 (s, 3H, $CH_3$ *i*Pr), 1.36–1.32 (m, 2H, $H_{cod}$), 1.15–1.05 (m, 1H, $H_{cod}$), 1.14–0.97 (m, 6H, $CH_2\underline{CH_3}$ Bodipy). $^{13}$C{$^1$H} NMR (126 MHz, methylene chloride-$d_2$) δ 180.0, 158.7, 154.9, 140.7, 135.9, 134.9, 134.0, 133.6, 132.3, 130.1, 123.7, 118.3, 86.5, 83.3, 71.1, 52.2, 36.7, 31.9, 31.3, 30.3, 27.8, 24.2, 23.7, 17.6, 14.8, 13.4, 13.0, 11.3, 10.0. $^{19}$F NMR (471 MHz, methylene chloride-$d_2$) δ −145.50 (dq, $J(^{11}B\text{-}^{19}F_a)$ = 33 Hz, $J(^{19}F\text{-}^{19}F)$ = 108 Hz), −146.03 (dq, $J(^{11}B\text{-}^{19}F_b)$ = 33 Hz, $J(^{19}F\text{-}^{19}F)$ = 108 Hz). HRMS (ESI positive): m/z calcd. for $C_{31}H_{43}BF_2IrN_4$: 713.31726 [M]; found 713.31873.

**[RhCl(cod)(3)]**. Complex [RhCl(cod)(**3**)] was obtained according to the general procedure A. **3**·HI (30 mg, 0.055 mmol), $Ag_2O$ (6.4 mg, 0.028 mmol), $[RhCl(cod)]_2$ (13.8 mg, 0.028 mmol) in 1,2-dichloroethane (2 mL) yields the complex as a dark red crystalline solid (8 mg, 22% yield). $^1$H NMR (500 MHz, methylene chloride-$d_2$) $^1$H NMR (500 MHz, methylene chloride-$d_2$) δ 7.19 (d, *J* = 1.7 Hz, 1H, CH), 7.03 (d, *J* = 1.4 Hz, 1H, CH), 6.12–6.04 (m, 1H, CH *i*Pr), 4.75–4.72 (m, 1H, $H_{cod}$), 4.69–4.65 (m, 1H, $H_{cod}$), 3.63–3.60 (m, 1H, $H_{cod}$), 3.14–3.11 (m, 1H, $H_{cod}$), 2.56 (s, 3H, $CH_3$ Bodipy), 2.51 (s, 3H, $CH_3$ Bodipy), 2.50–2.43 (m, 1H, $H_{cod}$), 2.38–2.31 (m, 4H), 2.26–2.19 (m, 1H, $H_{cod}$), 2.09–(m, 2H, $H_{cod}$), 1.93–1.87 (m, 1H, $H_{cod}$), 1.82–1.76 (m, 1H, $H_{cod}$), 1.72 (s, 3H, $CH_3$ *i*Pr), 1.70–1.67 (m, 1H, $H_{cod}$), 1.64–1.59 (m, 1H, $H_{cod}$), 1,56 (s, 3H, $CH_3$ Bodipy), 1.43 (s, 3H, $CH_3$ Bodipy), 1.33 (s, 3H, $CH_3$ *i*Pr), 1.03–0.96 (m, 6H, $CH_2\underline{CH_3}$ Bodipy).$^{13}$C{$^1$H} NMR (126 MHz, methylene chloride-$d_2$) δ 182.8 (d, *J* = 52.2 Hz), 159.0, 154.7, 141.2, 135.7, 135.0, 134.3, 133.6, 132.3, 129.9, 124.1, 118.5, 99.2, 97.2, 79.2 (d, *J* = 13.9 Hz), 70.6 (d, *J* = 14.4 Hz), 68.3 (d, *J* = 14.0 Hz), 60.8, 35.9, 31.4, 31.2, 30.5, 27.5, 24.3, 23.7, 21.3, 17.5 (d, *J* = 8.6 Hz), 14.9 (d, *J* = 7.1 Hz), 11.5, 9.8. $^{19}$F NMR (471 MHz, methylene chloride-$d_2$) δ −145.58 (dq, $J(^{11}B\text{-}^{19}F_a)$ = 33 Hz, $J(^{19}F\text{-}^{19}F)$ = 108 Hz), −145.91 (dq, $J(^{11}B\text{-}^{19}F_b)$ = 33 Hz, $J(^{19}F\text{-}^{19}F)$ = 104 Hz). HRMS (ESI positive): m/z calcd. for $C_{31}H_{43}BF_2N_4Rh$: 623.25984 [M]; found 623.26046.

**[PdCl(allyl)(3)]**. Complex [PdCl(allyl)(**3**)] was obtained according to the general procedure A. **3**·HI (30 mg, 0.055 mmol), $Ag_2O$ (6.4 mg, 0.028 mmol), $[PdCl(allyl)]_2$ (10.2 mg, 0.028 mmol) in 1,2-dichloroethane (2 mL) yields the complex as a dark red crystalline solid (8 mg, 25% yield). $^1$H NMR (500 MHz, chloroform-*d*) δ 7.29 (d, *J* = 1.9 Hz, 1H, CH), 7.09 (d, *J* = 1.9 Hz, 1H, CH), 5.57–5.49 (m, 1H, CH *i*Pr), 5.17–5.09 (m, 1H, allyl), 4.16–4.14 (m, 1H, allyl), 3.14 (d, *J* = 13.5 Hz, 1H, allyl), 3.08 (d, *J* = 6.7 Hz, 1H, allyl), 2.52 (d, *J* = 7.1 Hz, 6H, $CH_3$ Bodipy), 2.42–2.25 (m, 4H, $\underline{CH_2}CH_3$ Bodipy), 2.16 (d, *J* = 12.0 Hz, 1H, allyl), 1.64 (s, 3H, $CH_3$ Bodipy), 1.57–1.50 (m, 9H, $CH_3$ Bodipy + $CH_3$ *i*Pr), 1.03–0.99 (m, 6H, $CH_2\underline{CH_3}$ Bodipy). $^{13}$C{$^1$H} NMR (126 MHz, chloroform-*d*) δ 181.5, 157.0, 156.7, 137.5, 133.9, 133.7, 133.5, 129.6, 129.3, 122.0, 118.4, 115.2, 73.2, 53.0, 50.1, 26.8, 23.64, 23.57, 16.91, 16.88, 14.4, 12.69, 12.65, 9.6, 9.4. $^{19}$F NMR (471 MHz, chloroform-*d*) δ −144.50 (dq, $J(^{11}B\text{-}^{19}F_a)$ = 33 Hz, $J(^{19}F\text{-}^{19}F)$ = 108 Hz), −145.89 (dq, $J(^{11}B\text{-}^{19}F_b)$ = 33 Hz, $J(^{19}F\text{-}^{19}F)$ = 108 Hz). HRMS (ESI positive): m/z calcd. for $C_{26}H_{36}BF_2N_4Pd$: 559.20305 [M]; found 559.20394.

**[CuCl(3)]**. Complex [CuCl(**3**)] was synthesized according to the general procedure A. **3**·HI (50 mg, 0.092 mmol), $Ag_2O$ (10.7 mg, 0.046 mmol), CuCl (9.2 mg, 0.092 mmol) in 1,2-dichloroethane (5 mL). Complex [CuCl(**3**)] was obtained as a red microcrystalline solid (22.7 mg, 48% yield). $^1$H NMR (500 MHz, chloroform-*d*) δ 7.27 (s, 1H, CH), 7.05 (s, 1H, CH), 5.02–4.97 (m, 1H, CH *i*Pr), 2.53 (s, 6H, $CH_3$ Bodipy), 2.32 (q, *J* = 7.5 Hz, 4H, $\underline{CH_2}CH_3$ Bodipy), 1.58 (d, *J* = 6.7 Hz, 6H), 1.45 (s, 6H, $CH_3$ Bodipy), 1.02 (t, *J* = 7.5 Hz, 6H, $CH_2\underline{CH_3}$ Bodipy). $^{13}$C{$^1$H} NMR (126 MHz, chloroform-*d*) δ 176.6, 157.8, 136.3, 134.4, 132.6, 129.1, 122.5, 118.6, 54.5, 27.0, 24.2, 17.2, 14.6, 13.0, 9.5. $^{19}$F NMR (471 MHz, chloroform-*d*) δ −144.23 (dq, $J(^{11}B\text{-}^{19}F_a)$ = 33 Hz, $J(^{19}F\text{-}^{19}F)$ = 108 Hz), −146.34 (dq, $J(^{11}B\text{-}^{19}F_b)$ = 33 Hz, $J(^{19}F\text{-}^{19}F)$ = 108 Hz). HRMS (ESI positive): m/z calcd. for $C_{46}H_{62}B_2CuF_4N_8$: 887.4516 [M]; found 887.4527.

**[MCl(CO)$_2$(3)] (M = Rh, Ir)** To a Schlenk flask equipped with a stirring bar and septa, the corresponding cod-complex and DCM (2 mL) were added. A balloon with CO was connected via cannula and CO was bubbled through the stirred solution for 30 min at room temperature. The volatiles were evaporated under reduced pressure, pentane (5 mL) was added, and the suspension was sonicated for 5 min. The solid material was filtered off and washed with another batch of pentane (2 × 5 mL).

Complex [RhCl(CO)$_2$(**3**)] was obtained as a dark red solid from [RhCl(cod)(**3**)] (12 mg, 84% yield). $^1$H NMR (500 MHz, methylene chloride-$d_2$) δ 7.36 (d, *J* = 1.8 Hz, 1H, CH), 7.20 (d, *J* = 1.7 Hz, 1H, CH), 5.52–5.45 (m, 1H, CH *i*Pr), 2.52 (s, 6H, $CH_3$ Bodipy), 2.34 (q, *J* = 7.6 Hz, 4H, $\underline{CH_2}CH_3$, Bodipy), 1.56–1.53 (m, 12H, $CH_3$ Bodipy + $CH_3$ *i*Pr), 0.98 (t, *J* = 7.6 Hz, 6H, $CH_2\underline{CH_3}$ Bodipy). $^{13}$C{$^1$H} NMR (126 MHz, methylene chloride-$d_2$) δ 185.9, 185.5, 182.8, 182.3, 176.1, 175.7, 157.9, 134.8, 133.4, 129.9, 124.2, 119.8, 23.8, 17.5, 14.6, 13.2, 10.4.$^{19}$F NMR (471 MHz, methylene chloride-$d_2$) δ −144.88 (dq, $J_{B\text{-}Fa}$ = 31 Hz, $J(^{19}F\text{-}^{19}F)$ = 108 Hz), −145.82 (dq, $J_{B\text{-}Fb}$ = 33 Hz, $J(^{19}F\text{-}^{19}F)$ = 108 Hz). HRMS (ESI positive): m/z calcd. for $C_{26}H_{34}BF_2N_5ORh$: 584.1874 [M + $CH_3CN$]; found 584.1876.

Complex [IrCl(CO)$_2$(**3**)] was obtained as a dark red solid from [IrCl(cod)(**3**)]( 10 mg, 78% yield). $^1$H NMR (500 MHz, methylene chloride-$d_2$) δ 7.40 (s, 1H, CH), 7.21 (s, 1H, CH), 5.50–5.45 (m, 1H, CH *i*Pr), 2.51 (s, 6H, $CH_3$ Bodipy), 2.33 (q, *J* = 7.5 Hz, 4H, $\underline{CH_2}CH_3$ Bodipy), 1.61–1.46 (m, 12H, $CH_3$ Bodipy + $CH_3$ *i*Pr), 0.98 (t, *J* = 7.6 Hz, 6H, $CH_2\underline{CH_3}$ Bodipy). $^{13}$C{$^1$H} NMR (126 MHz, methylene chloride-$d_2$) δ 207.1, 180.9, 174.8, 168.2, 158.1, 135.0, 133.2, 124.4, 120.0, 30.5, 23.9, 17.7, 14.8, 13.5, 10.6. $^{19}$F NMR (471 MHz, methylene chloride-$d_2$) δ −144.83 (dq, $J_{B\text{-}Fa}$ = 33 Hz, $J(^{19}F\text{-}^{19}F)$ = 108 Hz), −145.82 (dq, $J_{B\text{-}Fb}$ = 31 Hz, $J(^{19}F\text{-}^{19}F)$ = 108 Hz). HRMS (ESI positive): m/z calcd. for $C_{25}H_{31}BF_2IrN_4O_2$: 661.2132 [M]; found 661.2141. *ν*(CO) 1971 and 2055 cm$^{-1}$.

**Photooxidation of *p–bromothioanisole***. Procedure: *p*-bromothioanisole (40.6 mg, 0.2 mmol), catalyst (0.002 mmol), 2-bromoanisole (internal standard, 24.9 μL, 0.2 mmol) were added into a 2 mL transparent vial and dissolved in 0.5 mL of *t*-amylalcohol and 0.5 mL of acetonitrile and the vial was irradiated under green LED. NMR was measured and the conversion to the product was calculated with respect to the internal standard.

**General procedure for the singlet oxygen generation and determination**. A mixture of 1,3-diphenylisobenzofuran (DPBF) (90 μM) and the respective photosensitizer (1.0 μM) was dissolved in the corresponding solvent (2 mL) and was irradiated under green LED light in a home-built photoreactor (supporting). The photooxidation of DPBF was monitored over time at time intervals depending on the efficiency (rate) of the photocatalytic reaction. The time-dependent absorption graphs show the decrease in the DPBF absorbance at 410 nm and the corresponding linear regression from which the rate was calculated. $\Phi_\Delta$ data

was obtained using 2,6-diiodo-Bodipy ($\Phi_\Delta = 0.75$ in $CH_3CN$) as the reference:[15a,41]

$$\Phi_\Delta = \Phi_\Delta^{st} \frac{r}{r^{st}} \frac{I^{st}}{I}$$

where ($r$) and ($r^{st}$) are the DPBF photooxidation rates in the presence of the corresponding photosensitizer (calculated from the decrease in absorbance at 410 nm), respectively; ($I$) and ($I^{st}$) are relative absorbance correction factors and were calculated according to the spectrum of the light source and the absorbance spectrum of the photosensitizer. Relative absorbance ($I$) allows translation of the experimental data from photosensitizers with different absorbance spectrums using a non-monochromatic light source for the irradiation.

$$I = \int_{484}^{600} i(\lambda)(1 - 10^{-A(\lambda)}) d(\lambda)$$

Where the integral of $i$, is the intensity of the light source at the specific wavelength ($\lambda$), with the corresponding absorbance value ($A$) at the given wavelength ($\lambda$).[42]

Deposition Number 2174553 (for [IrCl(CO)$_2$(**3**)]) contains the supplementary crystallographic data for this paper. These data are provided free of charge by the joint Cambridge Crystallographic Data Centre and Fachinformationszentrum Karlsruhe Access Structures service www.ccdc.cam.ac.uk/structures.

## Acknowledgements

*This work was supported by the Deutsche Forschungsgemeinschaft (DFG) via grant PI 178/18-2. We wish to thank Heraeus GmbH und Co.KG for a generous gift of $HAuCl_4$. Open Access funding enabled and organized by Projekt DEAL.*

## Conflict of Interest

The authors declare no conflict of interest.

## Data Availability Statement

The data that support the findings of this study are available in the supplementary material of this article.

**Keywords:** Gold · Iridium · NHC ligands · Singlet oxygen · Photooxidation

[1] P. Kos, H. Plenio, *Chem. Eur. J.* **2015**, *21*, 1088–1095.
[2] P. Kos, H. Plenio, *Angew. Chem. Int. Ed.* **2015**, *54*, 13293–13296; *Angew. Chem.* **2015**, *127*, 13491–13494.
[3] R. Vasiuta, H. Plenio, *Chem. Eur. J.* **2016**, *22*, 6353–6360.
[4] O. Halter, J. Spielmann, Y. Kanai, H. Plenio, *Organometallics* **2019**, *38*, 2138–2149.
[5] J. R. Lakowicz, *Principles of Fluorescence Spectroscopy*, Springer-Verlag, New York, **2010**.
[6] a) O. Halter, R. Vasiuta, I. Fernández, H. Plenio, *Chem. Eur. J.* **2016**, *22*, 18066–18072; b) T. Ueno, Y. Urano, K.-I. Setsukinai, H. Takakusa, H. Kojima, K. Kikuchi, K. Ohkubo, S. Fukuzumi, T. Nagano, *J. Am. Chem. Soc.* **2004**, *126*, 14079–14085; c) Y. Urano, M. Kamiya, K. Kanda, T. Ueno, K. Hirose, T. Nagano, *J. Am. Chem. Soc.* **2005**, *127*, 4888–4894.
[7] J. Zhao, K. Xu, W. Yang, Z. Wang, F. Zhong, *Chem. Soc. Rev.* **2015**, *44*, 8904–8939.
[8] M. A. Filatov, *Org. Biomol. Chem.* **2020**, *18*, 10–27.
[9] T. Yogo, Y. Urano, Y. Ishitsuka, F. Maniwa, T. Nagano, *J. Am. Chem. Soc.* **2005**, *127*, 12162–12163.
[10] M. A. Filatov, S. Karuthedath, P. M. Polestshuk, H. Savoie, K. J. Flanagan, C. Sy, E. Sitte, M. Telitchko, F. Laquai, R. W. Boyle, M. O. Senge, *J. Am. Chem. Soc.* **2017**, *139*, 6282–6285.
[11] K. X. Teng, W. K. Chen, L. Y. Niu, W. H. Fang, G. Cui, Q. Z. Yang, *Angew. Chem. Int. Ed.* **2021**, *60*, 19912–19920.
[12] Y. Dong, A. A. Sukhanov, J. Zhao, A. Elmali, X. Li, B. Dick, A. Karatay, V. K. Voronkova, *J. Phys. Chem. C* **2019**, *123*, 22793–22811.
[13] a) F. Geist, A. Jackel, R. F. Winter, *Inorg. Chem.* **2015**, *54*, 10946–10957; b) P. Irmler, R. F. Winter, *Dalton Trans.* **2016**, *45*, 10420–10434.
[14] M. T. Whited, P. I. Djurovich, S. T. Roberts, A. C. Durrell, C. W. Schlenker, S. E. Bradforth, M. E. Thompson, *J. Am. Chem. Soc.* **2011**, *133*, 88–96.
[15] a) D. Wang, R. Malmberg, I. Pernik, S. K. K. Prasad, M. Roemer, K. Venkatesan, T. W. Schmidt, S. T. Keaveney, B. A. Messerle, *Chem. Sci.* **2020**, *11*, 6256–6267; b) D. Wang, I. Pernik, S. T. Keaveney, B. A. Messerle, *ChemCatChem* **2020**, *12*, 5091–5097.
[16] A. M. Potocny, J. J. Teesdale, A. Marangoz, G. P. A. Yap, J. Rosenthal, *Inorg. Chem.* **2019**, *58*, 5042–5050.
[17] a) L. K. McKenzie, H. E. Bryant, J. A. Weinstein, *Coord. Chem. Rev.* **2019**, *379*, 2–29; b) M. Üçüncü, E. Karakuş, E. Kurulgan Demirci, M. Sayar, S. Dartar, M. Emrullahoğlu, *Org. Lett.* **2017**, *19*, 2522–2525.
[18] X.-F. Zhang, X. Yang, B. Xu, *Phys. Chem. Chem. Phys.* **2017**, *19*, 24792–24804.
[19] a) L. Gourdon, K. Cariou, G. Gasser, *Chem. Soc. Rev.* **2022**, *51*, 1167–1195; b) R. Prieto-Montero, A. Prieto-Castaneda, R. Sola-Llano, A. R. Agarrabeitia, D. Garcia-Fresnadillo, I. Lopez-Arbeloa, A. Villanueva, M. J. Ortiz, S. de la Moya, V. Martinez-Martinez, *Photochem. Photobiol.* **2020**, *96*, 458–477; c) S. Popov, H. Plenio, *Eur. J. Inorg. Chem.* **2021**, *22*, 3708–3718; d) B. Bertrand, K. Passador, C. Goze, F. Denat, E. Bodio, M. Salmain, *Coord. Chem. Rev.* **2018**, *358*, 108–124.
[20] D. J. Nelson, *Eur. J. Inorg. Chem.* **2015**, 2012–2027.
[21] E. A. Martynova, N. V. Tzouras, G. Pisanò, C. S. J. Cazin, S. P. Nolan, *Chem. Commun.* **2021**, *57*, 3836–3856.
[22] S. Leuthäußer, D. Schwarz, H. Plenio, *Chem. Eur. J.* **2007**, *13*, 7195–7203.
[23] This is necessary, since the recorded ATR-IR frequencies are shifted significantly relative to the traditional transmission IR frequencies and furthermore also differ from one ATR-IR spectrometer to another one - depending on the nature of the detector and window material.
[24] G. Ciancaleoni, N. Scafuri, G. Bistoni, A. Macchioni, F. Tarantelli, D. Zuccaccia, L. Belpassi, *Inorg. Chem.* **2014**, *53*, 9907–9916.
[25] S. Wolf, H. Plenio, *J. Organomet. Chem.* **2009**, *694*, 1487–1492.
[26] H. V. Huynh, *Chem. Rev.* **2018**, *118*, 9457–9492.
[27] G. Sheldrick, *Acta Crystallogr. Sect. A* **2015**, *71*, 3–8.
[28] O. V. Dolomanov, L. J. Bourhis, R. J. Gildea, J. A. K. Howard, H. Puschmann, *J. Appl. Crystallogr.* **2009**, *42*, 339–341.
[29] a) R. D. Savka, H. Plenio, *J. Organomet. Chem.* **2012**, *710*, 68–74; b) R. A. Kelly, H. Clavier, S. Giudice, N. M. Scott, E. D. Stevens, J. Bordner, I. Samardjiev, C. D. Hoff, L. Cavallo, S. P. Nolan, *Organometallics* **2008**, *27*, 202–210.
[30] A packing effect is unlikely, since DFT calculations reproduce the tilting of the two planes.
[31] a) O. Halter, I. Fernández, H. Plenio, *Chem. Eur. J.* **2017**, *23*, 711–719; b) O. Halter, H. Plenio, *Chem. Commun.* **2017**, *53*, 12461–12464.
[32] O. Halter, H. Plenio, *Eur. J. Inorg. Chem.* **2018**, 2935–2943.
[33] Y. You, *Org. Biomol. Chem.* **2018**, *16*, 4044–4060.
[34] a) W. Hu, M. Liu, X.-F. Zhang, M. Shi, M. Jia, X. Hu, L. Liu, T. Wang, *J. Phys. Chem. C* **2020**, *124*, 23558–23566; b) F. Wilkinson, J. G. Brummer, *J. Phys. Chem. Ref. Data* **1981**, *10*, 809–899.
[35] a) S. Xu, Y. Yuan, X. Cai, C.-J. Zhang, F. Hu, J. Liang, G. Zhang, D. Zhang, B. Liu, *Chem. Sci.* **2015**, *6*, 5824–5830; b) Y.-L. Chen, S.-W. Li, Y. Chi, Y.-M. Cheng, S.-C. Pu, Y.-S. Yeh, P.-T. Chou, *ChemPhysChem* **2005**, *6*, 2012–2017; c) P.-T. Chou, Y. Chi, M.-W. Chung, C.-C. Lin, *Coord. Chem. Rev.* **2011**, *255*, 2653–2665.
[36] W. H. Lam, E. S.-H. Lam, V. W.-W. Yam, *J. Am. Chem. Soc.* **2013**, *135*, 15135–15143.
[37] a) H. Plenio, M. Bergmann, M. Egert, *Chem. Eur. J.* **2017**, *23*, 13328–13331; b) M. Bergmann, H. Plenio, *Eur. J. Inorg. Chem.* **2018**, 2054–2059.

Research Article
doi.org/10.1002/ejic.202200335



[38] a) C. Bian, A. K. Singh, L. Niu, H. Yi, A. Lei, *Asian J. Org. Chem.* **2017**, *6*, 386–396; b) C. Ye, Y. Zhang, A. Ding, Y. Hu, H. Guo, *Sci. Rep.* **2018**, *8*, 2205; c) H. Guo, H. Xia, X. Ma, K. Chen, C. Dang, J. Zhao, B. Dick, *ACS Omega* **2020**, *5*, 10586–10595.
[39] a) C. Schiwek, J. Meiners, M. Förster, C. Würtele, M. Diefenbach, M. C. Holthausen, S. Schneider, *Angew. Chem. Int. Ed.* **2015**, *54*, 15271–15275; *Angew. Chem.* **2015**, *127*, 15486–15490; b) M. Selke, C. S. Foote, *J. Am. Chem. Soc.* **1993**, *115*, 1166–1167.
[40] The Vaska complex posseses two donating phosphine ligands and only single electron-withdrawing CO.
[41] A. M. Durantini, L. E. Greene, R. Lincoln, S. R. Martinez, G. Cosa, *J. Am. Chem. Soc.* **2016**, *138*, 1215–1225.
[42] L. V. Lutkus, S. S. Rickenbach, T. M. McCormick, *J. Photochem. Photobiol. A* **2019**, *378*, 131–135.

Manuscript received: May 25, 2022
Revised manuscript received: July 21, 2022